

Ultrathin-Layer $(\text{AlAs})_m(\text{GaAs})_m$ Superlattices with $m = 1, 2, 3$ Grown by Molecular Beam Epitaxy

T. Isu*, De-Sheng Jiang**, and K. Ploog

Max-Planck-Institut für Festkörperforschung, Heisenbergstrasse 1, D-7000 Stuttgart 80, Fed. Rep. Germany

Received 27 December 1986/Accepted 15 January 1987

Abstract. Ultrathin-layer $(\text{AlAs})_m(\text{GaAs})_m$ superlattices with $m = 1, 2,$ and 3 were grown by molecular beam epitaxy and characterized by x-ray diffraction and photoluminescence measurements. The appearance of distinct satellite peaks around the Bragg reflections demonstrate the formation of high-quality layered crystals. The observed luminescence shows a maximum at 2.033 eV for $m = 3$, and the emission energy decreases for $m = 2$ and $m = 1$ as well as for the $m = 4$ superlattice. This result for the monolayer superlattice is in good agreement with recent theoretical calculations, and it shows that the $(\text{AlAs})_1(\text{GaAs})_1$ superlattice represents a new artificial semiconductor material with novel electronic properties.

PACS: 68.55, 78.65, 78.70

The recent advances in the epitaxial growth techniques of molecular beam epitaxy (MBE) [1] and metal-organic vapour phase epitaxy (MO VPE) [2] allow the engineering of compound semiconductors on a molecular scale. High-quality superlattices comprised of ultrathin layers of AlAs and GaAs have been prepared with the superlattice period ranging from a value much larger than the underlying natural periodicity of the lattice down to the ultimate width of monolayers, where a monolayer is defined as one layer of cations plus one layer of anions [3]. In particular, the monolayer to several monolayer superlattices are of great current interest, because the electronic structure cannot be described by a combination of the two constituent semiconductors in terms of the effective mass theory [4, 5]. The compound semiconductor superlattices $(\text{AX})_m(\text{BX})_n$ with $m, n \leq 4$ can be considered as a new artificial semiconductor material with a variety of new electrical and optical properties. One of the intriguing features of these monolayer superlattices

should be the absence of alloy scattering which is dominant in the conventional ternary alloys $\text{Al}_{0.5}\text{Ga}_{0.5}\text{As}$ and $\text{Ga}_{0.47}\text{In}_{0.53}\text{As}$ [6].

In this paper we describe the growth of ultrathin-layer $(\text{AlAs})_m(\text{GaAs})_m$ superlattices with $m = 1, 2,$ and 3 by molecular beam epitaxy and their characterization by x-ray diffraction and low-temperature photoluminescence measurements. The growth rates of AlAs and GaAs monolayers were accurately controlled by the period of the intensity oscillations of the specularly reflected beam in the reflection high energy electron diffraction (RHEED) pattern, and actuation of the effusion cell shutters was synchronized to these oscillations. The occurrence of distinct satellite peaks around the (002) and the (004) reflections of the x-ray diffraction patterns confirms the formation of high-quality layered crystals. The luminescence peak energy obtained from these $(\text{AlAs})_m(\text{GaAs})_m$ superlattices exhibits a pronounced maximum at 2.033 eV for $m = 3$, and it decreases for the samples with $m = 2$ and $m = 1$ as well as for the $m = 4$ superlattice. This result for the $(\text{AlAs})_1(\text{GaAs})_1$ superlattice is in contrast to previous results by Ishibashi et al. [2], but it is in good agreement with the theoretical calculations of Nakayama and Kamimura [4] and Gell et al. [5] and

* On leave from Mitsubishi Electric Corp., Central Research Laboratory, Amagasaki, Hyogo 661, Japan

** On leave from Institute of Semiconductors, Academia Sinica, Beijing, PR China

with recent ellipsometric measurements [7]. The ultrathin-layer $(\text{AlAs})_m(\text{GaAs})_m$ superlattices with $m < 4$ indeed represent a new artificial semiconductor material with novel electronic properties.

1. Superlattice Growth

The ultrathin-layer $(\text{AlAs})_m(\text{GaAs})_m$ superlattices were grown in a three-chamber MBE system of the quasi-horizontal evaporation type which comprises a continuously rotating substrate holder for 2-inch diameter wafers and a liquid-nitrogen shroud encircling the growth region [8]. The superlattices were deposited on (001) oriented undoped semi-insulating GaAs substrates with a typical etch pitch density of $5 \times 10^4 \text{ cm}^{-2}$, using a growth temperature of $T_s < 550^\circ\text{C}$ and a growth rate as low as 1 monolayer per 5 s. For the present study the substrate rotation was not employed so that a deviation of $\pm 5\%$ from the ideal $\text{Al}_{0.5}\text{Ga}_{0.5}\text{As}$ stoichiometry across a 20-mm wafer area resulted. The contamination-free substrate surface was prepared by the cleaning method described in [8]. In brief, the etch-polished GaAs wafer was simply treated with concentrated H_2SO_4 and the stable surface oxide for passivation was generated by heating the wafer to 300°C in air under dust-free conditions for about 3 min. The surface oxide was then thermally desorbed by heating to 550°C in a flux of arsenic under ultrahigh vacuum conditions. A clear (2×4) surface reconstruction was observed in the RHEED pattern when the desorption process was finished. A $0.5 \mu\text{m}$ thick GaAs buffer layer was grown first on the heat-cleaned substrate to provide an atomically flat starting surface.

Prior to the growth of the superlattices, the growth rates of AlAs and of GaAs were determined accurately from the period of the intensity oscillations of the specular beam in the RHEED pattern, which was monitored by a photodiode. It is now well established that the intensities of the specularly reflected and of various diffracted beams of the RHEED pattern oscillate during MBE growth and that the period of these oscillations correspond exactly to the growth of a monolayer [9, 10]. The thickness of the AlAs and GaAs layers in the superlattice can thus be controlled by synchronizing the actuation of the respective effusion cell shutters with the RHEED oscillations. The low growth rate of 1 monolayer per 5 s for AlAs and for GaAs, which we used for the present study, ensured that the crystal growth occurs indeed in a two-dimensional layer-by-layer growth mode.

In Fig. 1 we show the RHEED intensity sequence for the $m=1$, $m=2$, and $m=3$ ultrathin-layer $(\text{AlAs})_m(\text{GaAs})_m$ superlattice. The synthesis of each superlattice period required four steps. At first a monolayer (or bi- or trilayer) of GaAs was deposited.

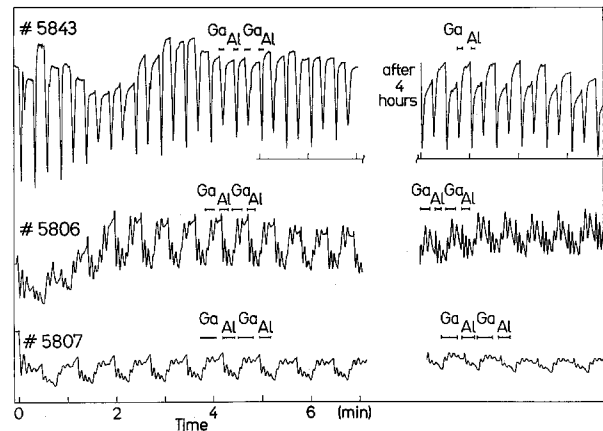


Fig. 1. RHEED intensity oscillations of specularly reflected electron beam from (001) surface in [100] azimuth during growth of $(\text{AlAs})_m(\text{GaAs})_m$ superlattices with $m=1, 2$, and 3

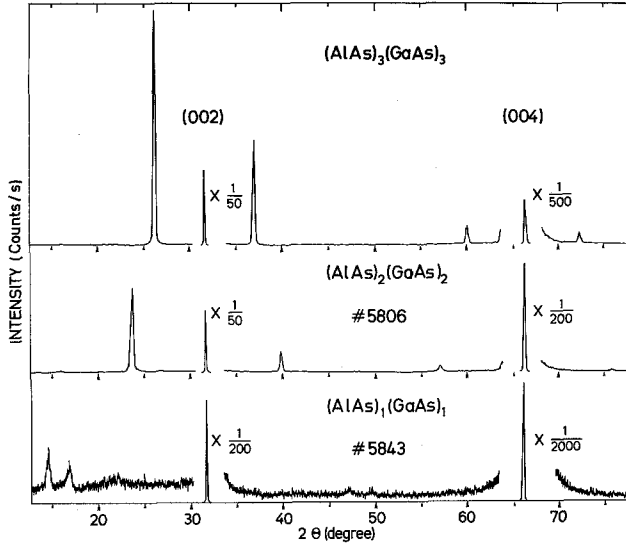
In the second step the crystal growth was stopped for 5 s and the surface was only exposed to the arsenic flux. The third step involved the deposition of a monolayer (or bi- or trilayer) of AlAs. Finally, the fourth step was the same as the second one. The shutters in front of the Ga and Al effusion cells, respectively, were opened at the time when the intensity of the specularly reflected beam had reached its maximum value and closed after one (or two or three) period(s). The maximum intensity indicated that the growth surface had become extremely smooth. The second and the fourth step of our growth sequence thus ensured that each layer was completed before the next one started. The four steps were repeated 500 times for the $m=1$ and $m=2$ superlattices and 400 times for the $m=3$ superlattice. Our detailed photoluminescence measurements on $(\text{AlAs})_m(\text{GaAs})_n$ superlattices with $m, n \geq 10$ have established that halting growth between successive periods does not adversely affect the optical properties of these multilayer structures. The cap layer of the superlattice was always formed by GaAs.

2. Determination of Superlattice Period by X-Ray Diffraction

The crystal quality and the superlattice period of the ultrathin-layer $(\text{AlAs})_m(\text{GaAs})_m$ superlattices were determined from x-ray rocking curves using a high-resolution double-crystal x-ray diffractometer [11] and also a counter diffractometer for a rapid scan over a wide range of diffraction angles. The diffraction patterns were recorded in the vicinity of the (002) and the (004) reflection using $\text{CuK}\alpha$ radiation. In Fig. 2 we show the measured x-ray diffraction curves for the $m=1, 2$, and 3 superlattices. In this figure the (002) peak at $\theta=15.81^\circ$ as well as the (004) peak at $\theta=33.0^\circ$

Table 1. Structural properties of ultrathin-layer (AlAs)_m(GaAs)_m superlattices obtained from x-ray diffraction measurements using CuK α radiation

Sample No.	Superlattice configuration	$\Delta\theta_{0,s}$ $\times 10^{-4}$ rad (004)	Average Al composition x	Satellite peak position				Period D [Å]	D/a
				(002)		(004)			
5843	(AlAs) ₁ (GaAs) ₁	-9.27	0.51	7.25	8.43	23.49	24.8	6.117	1.08
5806	(AlAs) ₂ (GaAs) ₂	-9.27	0.51		11.83	19.87	28.45 37.88	11.35	2.01
5807	(AlAs) ₃ (GaAs) ₃	-8.81	0.49		13.73	18.55	30.25 36.73	17.14	3.03

Fig. 2. X-ray diffraction patterns of (AlAs)_m(GaAs)_m superlattices with $m=1, 2,$ and 3 obtained in the vicinity of the (002) and (004) Bragg reflections using CuK α radiation

originate from both the epitaxial layer and the substrate. The weak (± 1) satellite reflections on the higher and lower angle side of these two Bragg reflections clearly indicate the existence of periodic structures. The period D of the (AlAs) _{m} (GaAs) _{m} superlattices can be determined from the angular distance between the zeroth-order (002) or (004) peak and the respective (\pm) satellite peaks using the equation

$$D = \frac{\lambda}{2|\sin\theta_{(\pm 1)} - \sin\theta_0|},$$

where λ is the x-ray wavelength and $\theta_{(\pm 1)}$ and θ_0 are the diffraction angles of the first-order satellite and of the zeroth-order reflection, respectively. Precise measurements of the angle separation $\Delta\theta_{0,s}$ between the substrate diffraction peak and the zeroth-order diffraction peak of the superlattice by means of the double-crystal x-ray diffractometer yielded the average value of the lattice constant and the average value of the Al composition x of the epitaxial layer (i.e., of the (AlAs) _{m} (GaAs) _{m} superlattice) by applying Vegard's rule

similar to the case of the ternary Al _{x} Ga _{$1-x$} As alloy [11]. In Table 1 we have summarized the structural data of the ultrathin-layer superlattices, as derived from the x-ray diffraction measurements. While for the $m=3$ and $m=2$ superlattices distinct (\pm) satellite peaks are located at the expected angular position, we observe a splitting of the satellite peaks for the $m=1$ superlattice. Two peaks appear around the ideal (001) position at $\theta=7.827^\circ$ ($2\theta=15.654^\circ$) as well as around the ideal (003) position at $\theta=24.11^\circ$ ($2\theta=48.22^\circ$). This splitting implies a slight deviation of the superlattice period D from the ideal twofold lattice constant a . From a careful evaluation of the RHEED intensity oscillation pattern depicted in Fig. 1 we assume that the period length of the (AlAs)₁(GaAs)₁ superlattice might be larger by about 5 to 8%, as compared to the ideal value of 5.659 Å. In this case each of the two satellite peaks located closer to the (002) and to the (004) reflection belongs to the respective zeroth order peaks as indicated in Table 1. Our detailed photoluminescence, Raman scattering [12] and ellipsometric measurements [7] revealed, however, that this slight deviation from ideality does not impose any falsification of the deduced optical properties of the (AlAs)₁(GaAs)₁ monolayer superlattice.

3. Luminescence Properties

The photoluminescence measurements were performed with the superlattice samples immersed in liquid He pumped to a temperature below 2 K. For excitation we used the 5300 Å (=2.34 eV) line of a cw Kr⁺ ion laser. The luminescence signal was analysed with a 1-m single-pass grating monochromator with slit widths of 0.2 and 0.3 mm, corresponding to a resolution of 2 and 2 Å, respectively, and detected by a GaAs cathode or S-1 cathode photomultiplier.

In Fig. 3 we show the low-temperature photoluminescence spectra obtained from the three prototype ultrathin-layer (AlAs) _{m} (GaAs) _{m} superlattices with $m=1, 2,$ and 3 . The three spectra are dominated by a strong luminescence line which strongly shifts in energy as a function of period length (i.e., of m). In

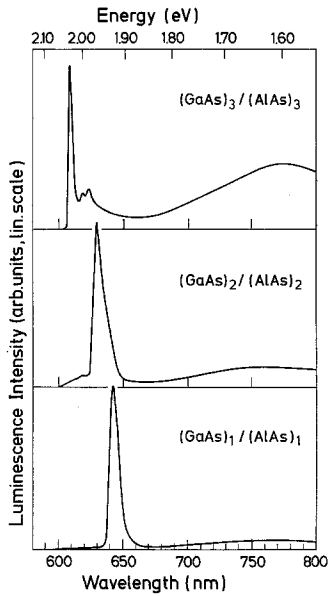


Fig. 3. Low-temperature photoluminescence spectra obtained from $(\text{AlAs})_m(\text{GaAs})_n$ superlattices with $m=1, 2$, and 3

Table 2. Variation of photoluminescence peak energy as a function of period length observed in ultrathin-layer $(\text{AlAs})_m(\text{GaAs})_n$ superlattices kept at 2 K. For comparison, also the energy of the bound-exciton luminescence detected in the ternary $\text{Al}_x\text{Ga}_{1-x}\text{As}$ alloy is included

Superlattice configuration	Average Al composition x	Luminescence peak energy [eV]
$(\text{AlAs})_1(\text{GaAs})_1$	0.51	1.931
$(\text{AlAs})_2(\text{GaAs})_2$	0.51	1.968
$(\text{AlAs})_3(\text{GaAs})_3$	0.49	2.033
$(\text{AlAs})_4(\text{GaAs})_4$	0.49	1.964
$\text{Al}_x\text{Ga}_{1-x}\text{As}$ alloy	0.52	2.077

Table 2 we have summarized the luminescence peak energies of the three superlattices. For comparison, we have also included the peak energy obtained from the $m=4$ superlattice and the bound-exciton line from the ternary $\text{Al}_x\text{Ga}_{1-x}\text{As}$ alloy. Although all five sample configurations were prepared under similar MBE growth conditions and have nearly the same average composition of $\text{Al}_{0.5}\text{Ga}_{0.5}\text{As}$, distinct differences exist in the peak position and in the line shape of the observed luminescence. The important result is that except for the ternary alloy the $m=3$ superlattice exhibits the highest luminescence peak energy of all $(\text{AlAs})_m(\text{GaAs})_m$ superlattices. In particular, the luminescence of the monolayer superlattice is shifted by 146 meV to lower energy as compared to the ternary $\text{Al}_{0.52}\text{Ga}_{0.48}\text{As}$ alloy. The observed dependence of the luminescence energy on the period length (i.e., on m) is in contrast to previous results of Ishibashi et al. [2], but

it is in good agreement with the theoretical calculations of Nakayama and Kamimura [4] and of Gell et al. [5] as well as with recent ellipsometric measurements [7]. Our results provide definite experimental evidence that the ultrathin-layer $(\text{AlAs})_m(\text{GaAs})_m$ superlattices with $m < 4$ indeed represent a new artificial semiconductor material with novel electronic properties.

The temperature and excitation intensity dependence of the photoluminescence spectra obtained from $(\text{AlAs})_m(\text{GaAs})_m$ superlattices with $m \leq 4$ clearly indicates the excitonic nature of the luminescence in these high-quality samples. Details of these measurements will be published elsewhere [13]. Inspection of Fig. 3 reveals that the $m=3$ superlattice exhibits the narrowest luminescence line with a halfwidth of $\Delta E \approx 12$ meV. The linewidth increases for the $m=2$ and $m=1$ superlattice. The reason for this line broadening is probably the increasing weight of the number of heterointerfaces on the luminescence properties when we go from $m=3$ to $m=1$. For the $m=3$ superlattice we further observe two weak phonon side bands at the low-energy side of the main peak. They are attributed to GaAs-like and AlAs-like LO-phonon side bands. We have detected such weak phonon side bands also in the photoluminescence spectra of $(\text{GaAs})_m(\text{AlAs})_n$ superlattices with $m, n > 4$ [13]. The occurrence of these side bands is related to zone folding effects and to the mixing of X and Γ states. It is noteworthy that for the ternary $\text{Al}_{0.52}\text{Ga}_{0.48}\text{As}$ alloy we observed two strong side bands with energy separations of 31 and 48 meV with respect to the 2.077 meV line, which are due to GaAs-like and AlAs-like LO-phonon coupling, respectively [13]. The intensities of these two side bands are comparable to or even stronger than the principal luminescence line. Such spectral features are characteristic for the indirect-gap ternary $\text{Al}_x\text{Ga}_{1-x}\text{As}$ alloy [14].

4. Conclusion

We have grown ultrathin-layer $(\text{AlAs})_m(\text{GaAs})_m$ superlattices with $m=1, 2$, and 3 by molecular beam epitaxy and we have characterized the samples by x-ray diffraction and by low-temperature photoluminescence measurements. The growth rates of AlAs and GaAs monolayers were accurately controlled by the period of the intensity oscillations of the specularly reflected beam in the RHEED pattern, and actuation of the Al and Ga effusion cell shutters was synchronized to these oscillations. The appearance of distinct satellite peaks around the (002) and (004) reflections of the x-ray diffraction patterns demonstrated the formation of high-quality layered crystals. The luminescence peak energy obtained from these superlattices

showed a pronounced maximum at 2.033 eV for $m=3$, and it decreased for the samples with $m=2$ and $m=1$ as well as for the $m=4$ superlattice. This result for the (AlAs)₁(GaAs)₁ monolayer superlattice is in contrast to previous experimental results [2], but it is in good agreement with recent theoretical calculations [4, 5]. The ultrathin-layer (AlAs)_m(GaAs)_m superlattices with $m < 4$ thus represent a new artificial semiconductor material with novel electronic properties.

Acknowledgments. We would like to thank A. Fischer for help with the sample preparation, L. Viczian for help with the x-ray measurements, W. Heinz for technical assistance with the photoluminescence measurements, and H. J. Queisser for critical reading of the manuscript. Part of this work was sponsored by the „Bundesministerium für Forschung und Technologie“ of the Federal Republic of Germany.

References

1. For reviews on recent developments see: *The Technology and Physics of Molecular Beam Epitaxy*, ed. by E.H.C. Parker (Plenum, New York 1985)
2. A. Ishibashi, Y. Mori, M. Itabashi, M. Watanabe: J. Appl. Phys. **58**, 2691 (1985)
3. A.C. Gossard, P.M. Petroff, W. Wiegmann, R. Dingle, A. Savage: Appl. Phys. Lett. **29**, 323 (1976)
4. T. Nakayama, H. Kamimura: J. Phys. Soc. Jpn. **54**, 4726 (1985)
5. M.A. Gell, D. Ninno, M. Jaros, D.C. Herbert: Phys. Rev. B **34**, 2416 (1986)
6. T. Yao: Jpn. J. Appl. Phys. **22**, L680 (1983)
7. M. Garriga, M. Cardona, N.E. Christensen, P. Lautenschlager, T. Isu, K. Ploog: Phys. Rev. B (submitted)
8. K. Ploog, A. Fischer: Appl. Phys. Lett. **48**, 1392 (1986)
9. J.H. Neave, B.A. Joyce, P.J. Dobson, N. Norton: Appl. Phys. A **30**, 1 (1983)
10. T. Sakamoto, H. Funabashi, K. Ohta, T. Nakagawa, N.J. Kawai, T. Kojima: Jpn. J. Appl. Phys. **23**, L 657 (1984)
11. L. Tapfer, K. Ploog: Phys. Rev. B **33**, 5565 (1986)
12. M. Cardona, T. Suemoto, N.E. Christensen, T. Isu, K. Ploog: Phys. Rev. B (submitted)
13. D.S. Jiang, K. Kelting, T. Isu, H.J. Queisser, K. Ploog: J. Appl. Phys. (submitted)
14. M.D. Sturge, E. Cohen, R.A. Logan: Phys. Rev. B **27**, 2362 (1983)